

Interference effects in the reaction $^{48}\text{Ti}(^{16}\text{O}, ^{15}\text{N})^{49}\text{V}$

G. B. Sherwood,* K. A. Erb, D. L. Hanson,[†] R. J. Ascutto, and D. A. Bromley
A. W. Wright Nuclear Structure Laboratory, Yale University, New Haven, Connecticut 06520

J. J. Kolata[‡]

Brookhaven National Laboratory, Upton, New York 11973

(Received 6 September 1978)

Anomalous angular distributions measured in the $^{48}\text{Ti}(^{16}\text{O}, ^{15}\text{N})^{49}\text{V}$ reactions, corresponding to population of a $3/2^-$ level at 0.153 MeV excitation, an $11/2^-$ level at 1.022 MeV and a $9/2^-$ level at 1.155 MeV, are analyzed by considering the interference effects of direct and indirect transfer processes. Within the weak-coupling model, the calculated population of these excited states in ^{49}V via pure two-step inelastic excitation and transfer is characterized by flat angular distributions, whereas a direct single-particle transfer yields a bell-shaped curve. Though neither of these processes taken individually is sufficient to account for the measured anomalous angular distributions associated with these levels, a coherent addition of contributions from both mechanisms results in the necessary interference. The consequent determination of the relative strengths of the competing routes indicates that the spectroscopic strengths of the directly populated single-particle components in the excited states are 2% or less.

NUCLEAR REACTIONS $^{48}\text{Ti}(^{16}\text{O}, ^{15}\text{N})^{49}\text{V}$; measured $\sigma(\theta)$. Enriched targets, resolution 90 keV; CCBA analysis of inelastic multistep contributions to $\sigma(\theta)$, using particle-core model for ^{49}V .

I. INTRODUCTION

A previous study of the $^{48}\text{Ti}(^{16}\text{O}, ^{15}\text{N})^{49}\text{V}$ reaction reported¹ several angular distributions which differed drastically from conventional distorted-wave Born approximation (DWBA) calculations, despite the qualitative, and sometimes quantitative, success of the DWBA for such reactions in this mass region.^{1,2} It was suggested in Ref. 1 that the anomalous angular distributions resulted from higher-order reaction processes, but as the spins, parities, and detailed structural properties of the ^{49}V levels in question were unknown at that time, no detailed analysis was possible.

Several factors have combined to motivate our present reexamination of the $^{48}\text{Ti}(^{16}\text{O}, ^{15}\text{N})^{49}\text{V}$ reaction. The spectroscopy of ^{49}V has now been studied extensively, and several levels have been identified which might be associated with the anomalous data of Ref. 1. However, the 250 keV energy resolution obtained in that work was insufficient to separate the various possible transitions, and thus higher resolution measurements were required. Moreover, recent studies³⁻⁶ of heavy-ion induced *two* nucleon transfer reactions have determined that anomalous angular distribution shapes similar to those observed in Ref. 1 can result when inelastic multistep amplitudes contribute strongly to the transfer process. In favorable situations, the interference occurring among the contributing reaction amplitudes has been shown to produce experimental signatures which probe otherwise inaccessible aspects of the nuclear

structure.

It is the purpose of the present work to identify and discuss the appearance of similar phenomena in a *one*-nucleon transfer reaction. We report a high resolution study of the $^{48}\text{Ti}(^{16}\text{O}, ^{15}\text{N})^{49}\text{V}$ reaction in which anomalous angular distributions are observed corresponding to population of the $\frac{3}{2}^-$, $\frac{11}{2}^-$, and $\frac{9}{2}^-$ levels at respective excitation energies of 0.153, 1.022, and 1.155 MeV in ^{49}V . Results of a full-recoil coupled-channels calculation incorporating both direct and inelastic multistep transfer are presented, and shown to account for the observed anomalies. Preliminary accounts of experimental⁷ and theoretical⁸ aspects of this work have appeared elsewhere.

II. EXPERIMENTAL PROCEDURE AND RESULTS

Angular distributions for the $^{48}\text{Ti}(^{16}\text{O}, ^{15}\text{N})^{49}\text{V}$ reaction were measured at a beam energy of 50 MeV, using the MP-7 accelerator and quadrupole-dipole-dipole-dipole spectrometer at the Brookhaven National Laboratory. The magnet was operated with a solid angle of 8 msr ($\Delta\theta = \pm 2.29^\circ$), and reaction products were detected by 5 cm \times 1 cm silicon position-sensitive focal plane counters. The targets consisted of thin (25–40 $\mu\text{g}/\text{cm}^2$) deposits of enriched ^{48}Ti (99.4%) evaporated onto 20 $\mu\text{g}/\text{cm}^2$ carbon backings. Absolute cross sections were determined by comparing the reaction yields with measurements of $^{16}\text{O} + ^{48}\text{Ti}$ elastic scattering at forward angles ($\theta_{\text{lab}} \leq 10^\circ$) where the scattering cross section is reproduced by the Rutherford ex-

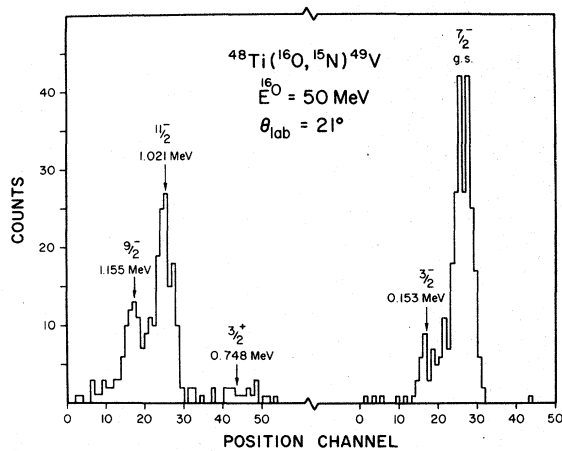


FIG. 1. Composite spectrum, consisting of data measured in two separate exposures, for the reaction $^{48}\text{Ti}(^{16}\text{O}, ^{15}\text{N})^{49}\text{V}$. The exposure for the left portion of the spectrum was about eight times longer than that for the low excitation-energy segment shown on the right.

pression.

A composite spectrum consisting of data measured in two separate runs is shown in Fig. 1. The exposure for the left portion of the spectrum was about eight times longer than that for the low excitation-energy segment shown on the right. An energy resolution of about 90 keV [fullwidth at half maximum (FWHM)] was obtained, which was

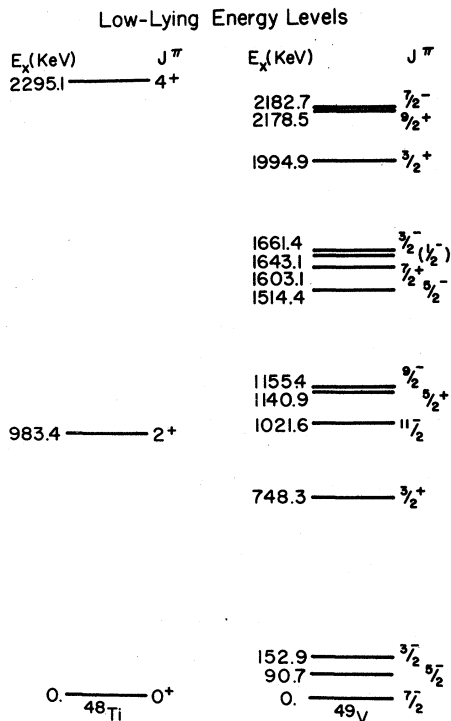


FIG. 2. Low-lying energy levels of ^{48}Ti and ^{49}V .

adequate for the study of most of the levels below 1.5 MeV excitation. Although the levels at 1.155 and 1.141 MeV shown in the ^{49}V level scheme of Fig. 2 were not resolved experimentally, the results of light-ion reaction studies support the interpretation of the yield observed near 1.15 MeV in Fig. 1 as arising from the population of the 1.155 MeV $9/2^-$ level. The large pickup strength for the neighboring 1.141 MeV $5/2^+$ level measured in the $^{50}\text{Cr}(t, \alpha)^{49}\text{V}$ reaction⁹ identifies the latter as a hole state, and the extremely weak population in the present work of the nearby $3/2^+$ hole

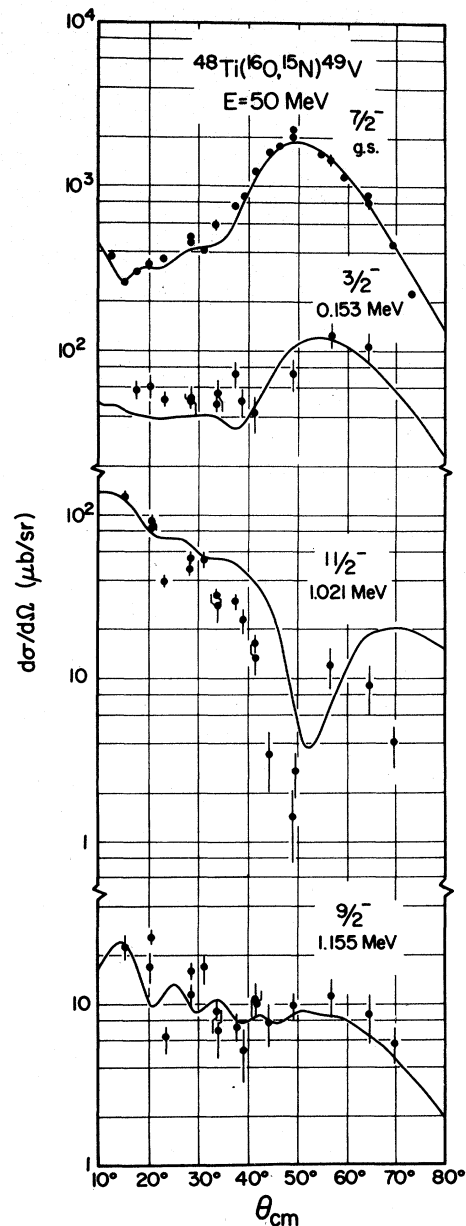


FIG. 3. Measured and calculated (CCBA) angular distributions for the reactions $^{48}\text{Ti}(^{16}\text{O}, ^{15}\text{N})^{49}\text{V}$.

state, at 0.748 MeV, provides empirical justification for assuming that the peak near 1.15 MeV corresponds to the $\frac{9}{2}^-$ level.

The measured angular distributions are shown in Fig. 3. The 50 MeV bombarding energy was chosen to ensure that direct, well-matched transitions would lead to normal, bell-shaped angular distributions. Such a shape is in fact observed for the ground state transition, which has a large spectroscopic strength for direct transfer. However, the measured angular distributions corresponding to population of the $\frac{3}{2}^-$, $\frac{11}{2}^-$, and $\frac{9}{2}^-$ states depart markedly from the normal bell shape, with features similar to those previously predicted and observed for heavy-ion *two-nucleon* transfer.³⁻⁶ In particular, we shall demonstrate that the enhanced width and forward peaking in the $\frac{9}{2}^-$ distribution result from dominant indirect transfer processes; that the deep minimum in the $\frac{11}{2}^-$ angular distribution is characteristic of destructive interference between direct and indirect processes; and that the $\frac{3}{2}^-$ data exhibit features characteristic of constructively interfering direct and indirect amplitudes.

III. REACTION AND STRUCTURE MODEL CONSIDERATIONS

The general shapes of these anomalous angular distributions point to probable contribution of inelastic multistep processes, judging by similarities to shapes observed in the study of heavy-ion two-nucleon transfer reactions. We have calculated the influence of such contributions in coupled-channels Born approximation (CCBA) by assuming a simple model for the structure of low-lying levels in ^{49}V . While the actual wave functions are undoubtedly different from—and more complicated than—those chosen here, the model discussed below permits a detailed and self-consistent investigation of the dynamics associated with competing

indirect transitions.

The lowest 2^+ -quadrupole vibrational state of ^{48}Ti has an excitation energy of 0.983 MeV and an enhanced $B(E2)$ with respect to the ^{48}Ti ground state.¹⁰ [$B(E2)$ values relevant to the present discussion are listed in Table I.] The two-proton particle, two-neutron hole structure of ^{48}Ti gives rise to additional collectivity as compared to the closed-shell ^{48}Ca system. The $\frac{11}{2}^-$ and $\frac{9}{2}^-$ states of ^{49}V have excitation energies close to that of the lowest quadrupole excitation in ^{48}Ti , and also have enhanced $B(E2)$ transitions connecting them to the ^{49}V ground state.¹¹⁻¹³ The excitation energies of these states have been calculated, using shell model ($f_{7/2}$)³ proton configurations, to be about 1 MeV.¹⁴ However, the resulting model wave functions lack the correlations necessary to describe the experimentally observed quadrupole collectivity of these states. Strong-coupling models also have been used to calculate excitation energies and reduced transition matrix elements for ^{49}V .^{11,12,15} Such calculations can approximate the excitation energies of the $\frac{11}{2}^-$ and $\frac{9}{2}^-$ states and do incorporate collective properties. An inadequacy again appears, however, when the number of extra-core protons is increased from one to three, in that the ground state spin is no longer correctly predicted.

A weak-coupling model is particularly convenient for incorporating, in an approximate way, nuclear structure considerations into the CCBA treatment of the various reaction processes. Thus we have chosen to describe low-lying levels of ^{49}V in terms of valence proton configurations coupled to the ground and first-excited states of the ^{48}Ti core:

$$\begin{aligned} |^{48}\text{Ti}(0^+) \rangle &= |0\rangle, \\ |^{48}\text{Ti}(2^+) \rangle &= \alpha_2^\dagger |0\rangle, \\ |^{49}\text{V}_{\text{g.s.}}(7/2^-) \rangle &= (d_{7/2}^\dagger |0\rangle), \\ |^{49}\text{V}(J^-) \rangle &= \{C_{\text{p.p.}}[(d_{7/2}^\dagger) \otimes \alpha_2^\dagger]_{J^-} + C_{\text{s.p.}}(d_{J^-}^\dagger)\} |0\rangle, \end{aligned} \quad (1)$$

TABLE I. Experimental reduced quadrupole transition probabilities for deexcitation of levels in ^{48}Ti and ^{49}V to the respective ground states.

E (keV)	^{48}Ti J^π	$B(E2)$ ($e^2\text{fm}^4$)	E (keV)	^{49}V J^π	$B(E2)$ ($e^2\text{fm}^4$)
983	2^+	138 ± 12^a	153	$\frac{3}{2}^-$	197 ± 20^b 197 ± 3^c
			1022	$\frac{11}{2}^-$	172 ± 59^c 144 ± 28^b
			1155	$\frac{9}{2}^-$	106 ± 28^c 58 ± 33^b

^aReference 7.

^bReference 8.

^cReference 9.

where $C_{p.p.}$ and $C_{s.p.}$ are the particle-phonon and single-particle components, respectively, $C_{p.p.}^2 + C_{s.p.}^2 = 1$, and α^\dagger and d^\dagger are the standard phonon and single-particle creation operators, respectively.

This weak-coupling model predicts a quintuplet of states with spins from $\frac{3}{2}$ to $\frac{11}{2}$ in the vicinity of 1 MeV excitation, whereas the closest experimental candidates for identification with these predicted states are spread over a considerable range of excitation energy in ^{49}V (Fig. 2). For the $\frac{9}{2}^-$ and $\frac{11}{2}^-$ members of the multiplet mixing can occur, in principle, with the $h_{9/2}$ or $h_{11/2}$ single-particle orbital of the $N=5$ oscillator shell. These components are expected to be small. The lowest $\frac{3}{2}^-$ state has an enhanced $B(E2)$, and is expected to mix appreciably with the $p_{3/2}$ single-particle orbital from the $N=3$ oscillator shell. No evidence was found for population of the $\frac{3}{2}^-$ state at 0.091 MeV in the experiment, but a weak transition comparable to that observed for other excited states would have been obscured in our spectra by the strong yield to the adjacent ground state.

Our nuclear structure model is admittedly simplistic when we consider that the ground state of ^{49}V should comprise three-particle, two-hole configurations. Nevertheless, the model has heuristic value since it allows us to study the reaction dynamics simply. *Within this model*, the nature of the interference between reaction mechanisms can be characterized by a single parameter ($C_{s.p.}/C_{p.p.}$), the amplitude ratio for the single-particle and particle-phonon components of the residual state. The direct (one-step) transfer process thus proceeds from the ground state of ^{48}Ti through the single-particle component of the excited state of ^{49}V , with a transfer amplitude proportional to $C_{s.p.}$. The indirect (two-step) transfer process populates only the particle-phonon component and has an amplitude proportional to $C_{p.p.}$. The following reduced matrix elements for transfer and inelastic scattering are implied by the model under consideration:

$$\begin{aligned} \langle ^{49}\text{V}(7/2^-) \| d_{7/2}^\dagger - \| ^{48}\text{Ti}(0^+) \rangle &= -\sqrt{8}, \\ \langle ^{49}\text{V}(J^-) \| d_{7/2}^\dagger - \| ^{48}\text{Ti}(0^+) \rangle &= -(2J+1)^{1/2} C_{s.p.}, \quad (2) \\ \langle ^{49}\text{V}(J^-) \| d_{7/2}^\dagger - \| ^{48}\text{Ti}(2^+) \rangle &= -(-1)^{7/2+2-J} (2J+1)^{1/2} C_{p.p.}, \\ \langle ^{48}\text{Ti}(2^+) \| \alpha_2^\dagger \| ^{48}\text{Ti}(0^+) \rangle &= \beta_2, \quad (3) \\ \langle ^{49}\text{V}(J^-) \| \alpha_2^\dagger \| ^{49}\text{V}(7/2^-) \rangle &= [(2J+1)/5]^{1/2} C_{p.p.} \beta_2. \end{aligned}$$

[The spectroscopic amplitude for transfer is given by the product of the matrix element and $(-1)^{(2J+1)^{-1/2}}$, i.e., the Racah phase convention is employed.] Inelastic excitation in the ^{16}O and ^{15}N systems was neglected, and the transfer processes were calculated with unit spectroscopic

strength for these systems.

Solution of the coupled equations included a full-recoil formulation for all the transitions. The indirect processes included both Coulomb and nuclear inelastic scattering. The various parameters that enter this analysis will be discussed in the following sections. Details of the calculations are given in Ref. 16.

IV. ANALYSIS

A. The ground state

Figure 4 shows the experimental angular distribution corresponding to the ^{49}V ground state together with various theoretical predictions. This transition is completely dominated by the direct transfer process since the ground state of ^{49}V has almost exclusive parentage with respect to the ^{48}Ti ground state. Starting with a four parameter optical-model potential which describes the elastic scattering of ^{16}O on ^{48}Ti at 48 MeV,¹ we calculate a bell-shaped angular distribution similar to that measured for the ground state, but which misses the grazing peak angle by a few degrees and which underestimates the experi-

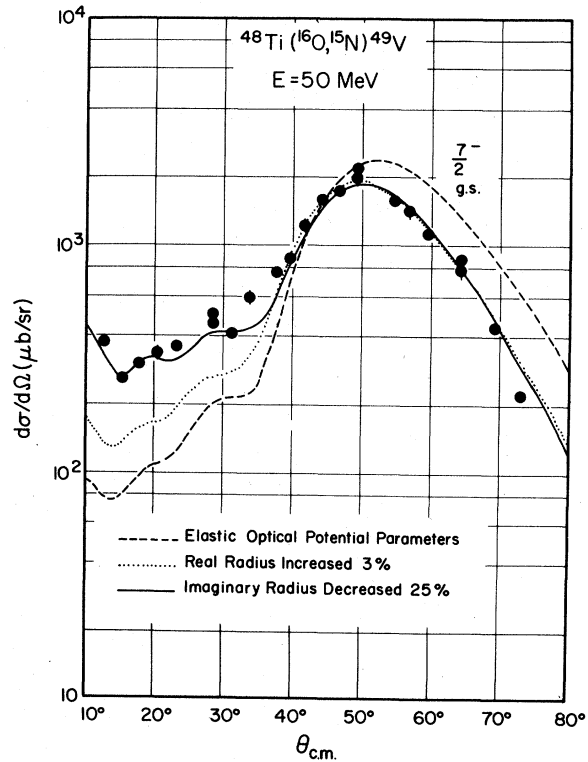


FIG. 4. A comparison of calculated (DWBA) angular distributions for the reaction $^{48}\text{Ti}(^{16}\text{O}, ^{15}\text{N})^{49}\text{V}(\frac{7}{2}^-, \text{g.s.})$ using different optical potential parameters. Parameters are discussed in the text and listed in Table II. The measured data are also plotted.

mental cross sections at forward angles. Both of these discrepancies have been encountered repeatedly in the study of heavy-ion reactions^{1,2,17,18} involving transitions dominated by a direct transfer process, and are believed to reflect an inadequacy in the simple optical-model parametrization; as such, they are not particularly relevant to the much greater departures from bell shape, which are observed for transitions to the excited states. The anomalous angular distributions associated with the $\frac{9}{2}^-$ and $\frac{11}{2}^-$ excited states also differ markedly from one another. Since the purpose of the present investigation is to understand the origin of these anomalous angular distributions, we have adjusted the optical potential parameters to obtain a fit to the angular distribution associated with the direct population of the $\frac{7}{2}^-$ ground state. This ground-to-ground transfer is then taken as an intermediate transition in the two-step population of the excited states.

There are a number of procedures which may be used to fit the experimental grazing peak. However, if we restrict ourselves to the variation of a single potential parameter the one we have found best to change is the imaginary radius. A reduction of 25% in both the entrance and exit channel imaginary radii reproduces the ground state angular distribution and gives the best fits to the excited state distributions, when all of the transfer routes are included. The resultant optical model potential parameters are listed in Table II. The common normalization factor for the solid curve in Fig. 4 and for the calculated angular distributions for the ^{49}V excited states is 0.9.

B. The excited states

Figure 5 shows calculated angular distributions for direct transfer (DWBA) to hypothetical single-particle states in ^{49}V . All of these predicted transitions are characterized by very similar bell-shaped angular distributions. There are minor differences, such as the damping of forward-angle oscillations as the spin of the residual state is increased, and there are predicted variations in transition strength. The differential cross section for population of the $\frac{3}{2}^-$ state is enhanced by the presence of an additional node in the bound-state wave function, while the population of the $\frac{9}{2}^-$

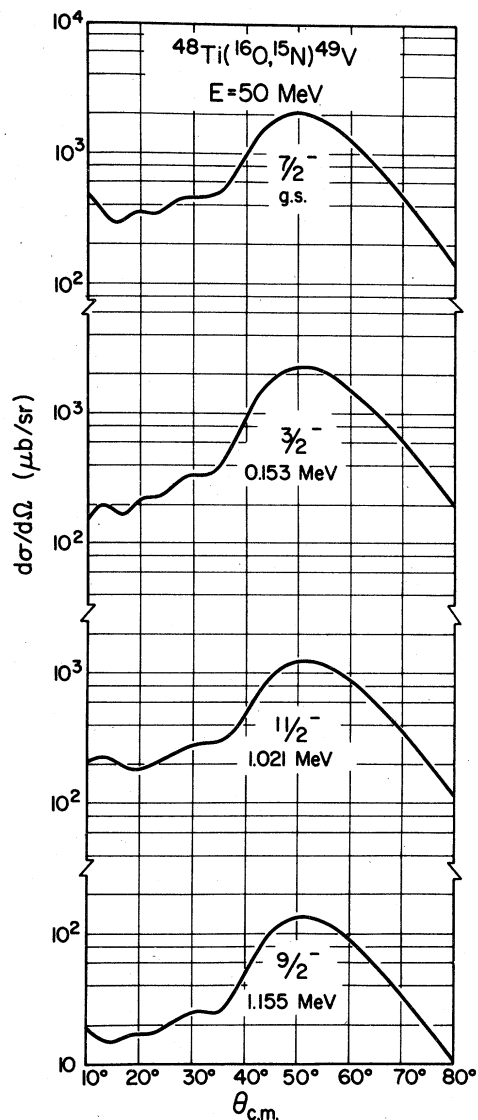


FIG. 5. Calculated direct transfer (DWBA) angular distributions for the $^{48}\text{Ti}(^{16}\text{O}, ^{15}\text{N})^{49}\text{V}$ reactions discussed in the text.

state is geometrically inhibited as compared to that of the $\frac{11}{2}^-$ state. However, such angular distributions—which are typical of direct transfers—cannot fit the experimental data associated with the ^{49}V excited states.

TABLE II. Optical model potential parameters used in the analysis.

	V (MeV)	W (MeV)	r_V (fm)	r_W (fm)	r_C (fm)	a_V (fm)	a_W (fm)
Scattering	100	40	1.22	0.915 ^a	1.2	0.5	0.5
Bound states			1.2		1.2	0.65	

^aReduced by 25% from elastic scattering value.

The two-step mechanisms which we employ consist of either inelastic excitation of the target nucleus followed by transfer, or transfer followed by inelastic excitation of the residual nucleus. Angular distributions for these two population routes to the $\frac{3}{2}^-$ state are denoted in Fig. 6 by the dashed and dotted curves, respectively. The nuclear and charge deformation parameters employed in all calculations were β_2 (nuc) = 0.230 and β_2 (charge) = 0.241. For this simple collective model, we have assumed that these parameters are the same in both the target and residual nuclei. The nuclear deformation parameter is consistent with that derived by Yntema and Satchler¹⁹ from α particle scattering on ^{48}Ti . The charge deformation parameter is obtained from the $B(E2)$ of ^{48}Ti as measured by Hausser, *et al.*¹⁰ We also assume that the particle transfer between two excited states can be described with the same form factor as that which is used for the ground state-to-ground state transfer. The actual nuclei will, of course, have properties which depart from such a simple, symmetric picture. Nevertheless, as shown in Fig. 6, and also in Fig. 8, the calculated two-step angular distributions have systematic differences depending on whether the particle transfer occurs between ground states or between excited states

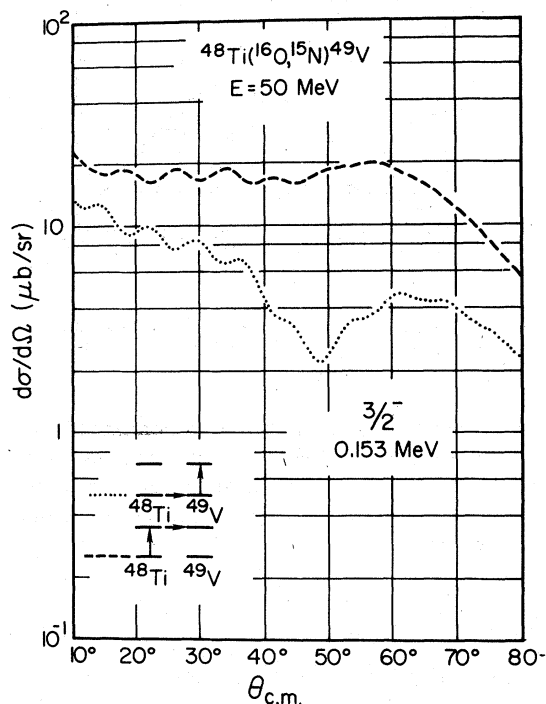


FIG. 6. Comparison of calculated (CCBA) angular distributions corresponding to population of the $\frac{3}{2}^-$ level at 0.153 MeV excitation, in the $^{48}\text{Ti}(^{16}\text{O}, ^{15}\text{N})^{49}\text{V}$ reaction, via the separate two-step routes shown.

in addition to the expected differences between these distributions and those of the direct, one-step routes.

In general, the shapes of the two-step angular distributions predicted in the model calculations are broad and forward peaked as compared to the bell shapes of the corresponding direct angular distributions. Such differences have been explained in terms of the corresponding S -matrix distributions in angular momentum space. The two-step processes tend to have narrower S -matrix distributions (corresponding to more intimate collisions), and consequently yield angular distributions characteristic of a relatively small number of partial waves. The shape differences between the different two-step distributions (e.g., Fig. 6) can be attributed to the fact that the effects of the inelastic excitation are more apparent when excitation is the latter of the two steps. Thus, the two-step route which includes the excitation of the residual nucleus yields a more forward peaked angular distribution in which the destructive, nuclear-Coulomb excitation minimum is more distinct, compared to the other two-step route. Such effects are apparent for the other excited states, but the differences between the two-step distributions become less pronounced as the spin of the

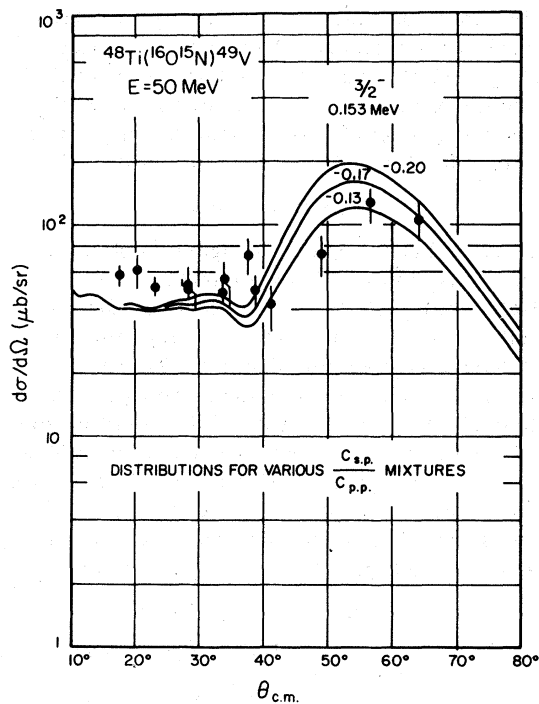


FIG. 7. Comparison of calculated (CCBA) angular distributions corresponding to population of the $\frac{3}{2}^-$ level at 0.153 MeV excitation, in the $^{48}\text{Ti}(^{16}\text{O}, ^{15}\text{N})^{49}\text{V}$ reaction, with various ratios of single-particle to particle-phonon mixtures.

residual nuclear state is increased (Fig. 8).

1. The $3/2^-$ state at 0.153 MeV

Angular distributions calculated with various direct-indirect contributions are compared in Fig. 7. The data contain a peak near the grazing angle, but the forward-angle cross sections are too large to be described by a purely direct transition. The magnitudes of these forward-angle yields are approximated instead by the indirect inelastic transfer. A small, direct admixture then allows the peak to be fitted. In this case, the interference between direct and indirect processes is found to be constructive. A sign difference between $C_{s.p.}$ and $C_{p.p.}$ is necessary to produce this result for the $3/2^-$ state. (Within our model, the two two-step routes corresponding to target and residual nucleus excitation interfere constructively with each other in the population of all three excited states, independent of the signs of the coefficient.)

2. The $9/2^-$ state at 1.155 MeV

Figure 8 shows angular distributions for the mechanisms populating the $9/2^-$ state. The combined, pure two-step angular distribution is broad, forward peaked, and oscillatory, as shown by the

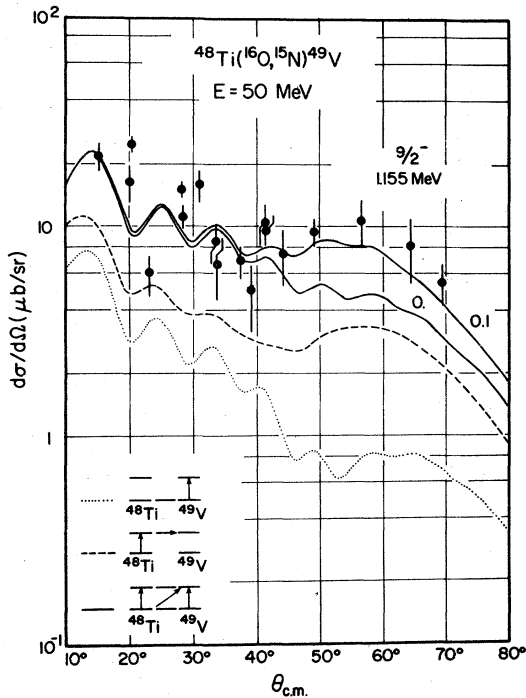


FIG. 8. Comparison of calculated (CCBA) angular distributions corresponding to population of the $9/2^-$ level at 1.155 excitation, in the $^{48}\text{Ti}(^{16}\text{O}, ^{15}\text{N})^{49}\text{V}$ reaction, via separate two-step routes and via their coherent sum (curve labeled 0.0). The curve labeled 0.1 includes a small direct component as discussed in the text.

solid curve labeled by $C_{s.p.}/C_{p.p.} = 0$. This calculation tends to underestimate the data at large angles, and a small single-particle component in the $9/2^-$ state would help to reproduce the data, as the curve labeled $C_{s.p.}/C_{p.p.} = 0.1$ indicates. However, this change in the calculated angular distribution is somewhat smaller than is the case for those corresponding to the $3/2^-$ and $11/2^-$ states, and there are uncertainties in the calculation which could affect the pure two-step distribution in such a way as to make a direct component in the reaction unnecessary. For example, the magnitude of the dashed route in Fig. 8 can be changed by a few percent depending upon whether the transfer form factor includes the $1f_{7/2}$ wave function bound with the proton separation energy from the ground state or from the excited state in ^{49}V . As mentioned previously, these calculations employ the same transfer form factors for the dotted and dashed routes; i.e., the separation energy from the ground state is used. In addition, the magnitude of the dotted route is uncertain to the extent that the deformation parameters for ^{49}V are different from those of ^{48}Ti . We have mentioned that the same deformation parameters were used for each nucleus. Some of the charge deformation

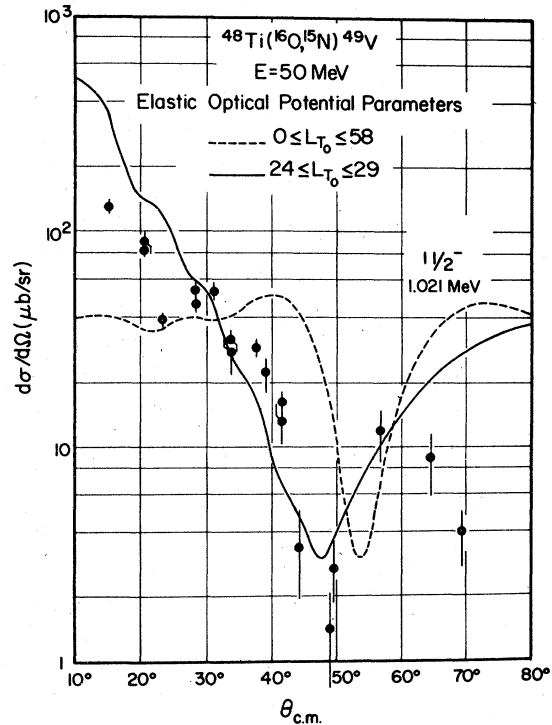


FIG. 9. Comparison of calculated (CCBA) angular distributions corresponding to population of the $11/2^-$ level at 1.021 MeV excitation in the $^{48}\text{Ti}(^{16}\text{O}, ^{15}\text{N})^{49}\text{V}$ reaction, with various ratios of single-particle to particle-phonon mixtures. The dashed curve illustrates the effects of introducing a complex phase between these components, as discussed in the text.

parameters recently deduced for ^{49}V are a few percent larger than the one used in this analysis (cf. Ref. 20). Finally we recall that the data shown in Fig. 8 may include small contributions from the nearby $\frac{3}{2}^+$ state.

3. The $11/2^-$ state at 1.022 MeV

Figure 9 shows various angular distributions resulting from the destructive interference between one- and two-step transfer processes leading to the $\frac{11}{2}^-$ state in ^{49}V . The curve labeled $C_{s.p.}/C_{p.p.} = 0$, displays the broad, forward-peaked shape expected from a pure two-step transfer. Its magnitude is correct at forward angles, but the shallow minimum near 47° , which is the result of destructive nuclear-Coulomb interference within the inelastic excitation, is not deep enough to reproduce that observed experimentally. However, as $C_{s.p.}$ is increased slightly, the required minima emerge in the calculated distributions, although the back-angle data points are overestimated. If $C_{s.p.}$ is then increased further, the bell-shaped distribution of a direct transfer appears. The intermediate value of the ratio $C_{s.p.}/C_{p.p.} \approx 0.15$ leads to a calculated angular distribution which qualitatively fits the data. Thus we conclude within the context of the present model that the $\frac{11}{2}^-$ level is populated through a combination of direct and indirect processes, which interfere destructively to form the sharp, deep minimum near the grazing angle.

The presence of such a deep minimum in the data represents a very strict test for the structure and reaction models, and consequently allows us to probe regions not usually accessible via purely direct reactions. The angular position of the minimum in the calculated distribution is not very sensitive to the $C_{s.p.}/C_{p.p.}$ ratio or to the parameters of the chosen optical potential. However, the minimum can be moved somewhat in angle through the artificial introduction of a complex phase between $C_{s.p.}$ and $C_{p.p.}$. As an example the dashed curve in this figure shows that the calculated minimum can be moved toward the experimental one if $C_{s.p.}$ is allowed to have a small negative imaginary part. This observation is not meant to imply that $C_{p.p.}$ or $C_{s.p.}$ should be complex. We might interpret this sensitivity as suggesting that the discrepancy of a few degrees in positioning the minimum reflects a deficiency in the reaction description, perhaps involving the form of the optical model parametrization.

In this regard, it is interesting to compare the angular distributions resulting from different sets of partial waves (Fig. 10). We have previously noted that the transfer angular distributions are

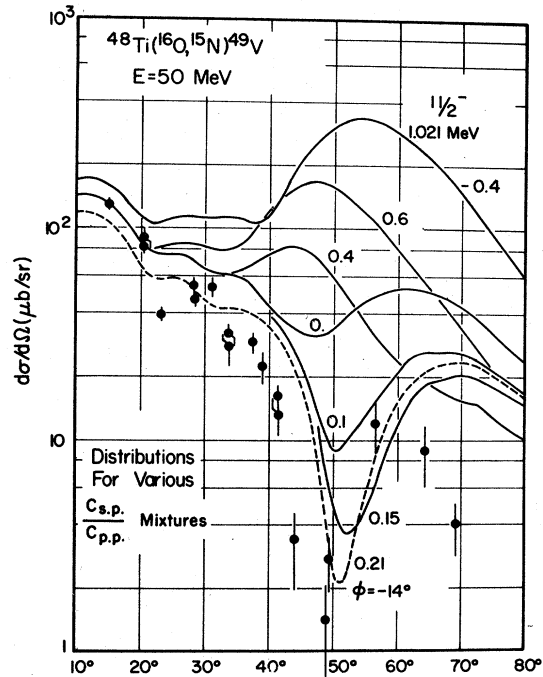


FIG. 10. Comparison of destructive interference angular distributions corresponding to population of the $\frac{11}{2}^-$ level at 1.021 MeV, in the $^{48}\text{Ti}(^{16}\text{O}, ^{15}\text{N})^{49}\text{V}$ reaction, for different sets of partial waves (total angular momenta). Elastic scattering potential parameters were used ($r_p = r_w = 1.22$ fm). The theoretical curves were individually normalized to the data.

fitted with a set of optical potential parameters which has a reduced imaginary radius compared to that which fits the elastic scattering cross section. This modification is presumably necessary to decrease the effect of scattering from small impact parameters compared to that from the surface region. However, there is an apparent confirmation of the "elastic" potential, at least as far as the surface partial waves are concerned. In Fig. 10 the dashed curve corresponds to a full calculation for the $\frac{11}{2}^-$ residual state. The calculated destructive interference minimum is positioned a few degrees back of the minimum in the data, in roughly the same position it would occupy were the imaginary radius reduced. The fit at forward angles is unsatisfactory, as it is for the dashed curve in Fig. 4. However, if only those partial waves which include the largest contributions from both the two-step and direct mechanisms are considered, the interference minimum is positioned correctly, as shown by the solid curve of Fig. 10. Moreover, deviations from the "elastic" potential tend to suppress the minimum within this truncated angular momentum space. These results indicate the need for an increasingly absorptive potential as the total angu-

TABLE III. Spectroscopic strengths for the direct population of several levels in ^{49}V . The results of the present CCBA investigation of the $^{48}\text{Ti}(^{16}\text{O}, ^{15}\text{N})^{49}\text{V}$ reaction are given in the third column. The fourth column lists the spectroscopic strengths which would be obtained from the present data if indirect reaction processes were to be neglected (DWBA analysis). The subsequent columns refer to previous reaction studies.

E (MeV)	J^π	$(2J+1)N'C^2_{s.p.}$ ($^{16}\text{O}, ^{15}\text{N}$)	($^{16}\text{O}, ^{15}\text{N}$)	$(2J+1)C^2S$ ($^{16}\text{O}, ^{15}\text{N}$) ^a	($^3\text{He}, d$) ^b	($^3\text{He}, d$) ^c
0.000	$\frac{7}{2}^-$	3.6	3.6	3.4	2.5	4.3
0.153	$\frac{3}{2}^-$	0.03	0.14	...	0.07	0.17
1.021	$\frac{11}{2}^-$	0.12	0.09-0.6
1.155	$\frac{5}{2}^-$	0.045	0.70

^aReference 1.

^bReference 23.

^cReference 9.

lar momentum of the system is decreased. The *ad hoc* L -dependent potential developed by Chatwin, *et al.*²¹ and the Gobbi-type²² surface-transparent potentials¹⁸ both have this property.

V. SUMMARY AND CONCLUSIONS

Angular distributions corresponding to the population of low-lying states in ^{49}V were measured in a high resolution study of the reaction $^{48}\text{Ti}(^{16}\text{O}, ^{15}\text{N})^{49}\text{V}$. Three levels, at excitation energies of 0.153 MeV, 1.022 MeV, and 1.155 MeV were weakly populated, and the associated angular distributions were found to differ significantly from the normal bell shape which is characteristic of direct reactions under comparable conditions.

We have analyzed and explained the anomalous angular distributions in terms of interference between direct and indirect reaction amplitudes. A very simple nuclear model has been employed to illustrate the dependencies of the angular distributions on these different reaction mechanisms, and the transfer has been found to be dominated by indirect processes. The spectroscopic strengths associated with the direct components of the transfer are listed in Table III. In the present CCBA model we have found that the calculations may be normalized to the data by choosing

$N'[2.0(C_{p.p.}^2 + C_{s.p.}^2)] = 0.9$, where a spectroscopic factor of two is assumed for the ^{16}O projectile. Thus, the constant N' is determined to be 0.45 for our calculations, and the spectroscopic factors for the directly populated components of the excited states are very small: $C_{s.p.}^2 \leq 0.02$. Larger components, in other nuclei with comparable deformations, could easily prevent observation of the competing two-step processes.

For comparison we also list in Table III spectroscopic strengths extracted from a DWBA analysis of the excited state data (assuming no indirect processes are involved). Excepting that for the $\frac{3}{2}^-$ reaction, these spectroscopic strengths are larger than can be encompassed in any structure model, and none of the measured excited state angular distribution shapes are reproduced by the DWBA calculations. We conclude that the multi-step processes are present and important in the $^{48}\text{Ti}(^{16}\text{O}, ^{15}\text{N})^{49}\text{V}$ reactions. The fitting of the general shapes of the excited state anomalous angular distributions, with the proper relative normalizations, presents a strong argument in favor of a reaction model which combines an interplay of nuclear structure and reaction dynamics of the type presented here.

This work was supported in part by the U. S. Department of Energy under Contract No. EY-76-C-02-3074.

*Present address: Bell Telephone Laboratories, Holmdel, New Jersey.

†Present address: Los Alamos Scientific Laboratory, Los Alamos, New Mexico.

‡Present address: Physics Department, University of Notre Dame, Notre Dame, Indiana.

¹J. V. Maher, K. A. Erb, and R. W. Miller, *Phys. Rev. C* **7**, 651 (1973).

²G. C. Morrison, H. J. Körner, L. R. Greenwood, and R. H. Siemssen, *Phys. Rev. Lett.* **28**, 1662 (1972); H. J. Körner, G. C. Morrison, L. R. Greenwood, and R. H. Siemssen, *Phys. Rev. C* **7**, 107 (1973), and references therein.

³R. J. Ascutto and N. K. Glendenning, *Phys. Lett.* **45B**, 85 (1973); R. J. Ascutto and J. S. Vaagen, in *Proceedings of the International Conference on Reactions*

- between *Complex Nuclei*, Nashville, Tennessee, 1974, edited by R. L. Robinson, F. K. McGowan, J. B. Ball, and J. H. Hamilton (North-Holland, Amsterdam, American Elsevier, New York, 1974), Vol. II, and references therein; N. K. Glendenning, *ibid.*, p. 137; R. J. Ascutto and N. K. Glendenning, *Phys. Lett.* **47B**, 332 (1973).
- ⁴K. A. Erb, D. L. Hanson, R. J. Ascutto, B. Sorensen, J. S. Vaagen, and J. J. Kolata, *Phys. Rev. Lett.* **33**, 1102 (1974).
- ⁵K. Yagi, D. L. Hendrie, L. Krauss, C. F. Maguire, J. Mahoney, D. K. Scott, Y. Terrien, T. Udagawa, K. S. Low, and T. Tamura, *Phys. Rev. Lett.* **34**, 96 (1975).
- ⁶R. J. Ascutto, J. S. Vaagen, D. J. Pisano, C. E. Thorn, J. R. Lien, and G. Løvholden, *Nucl. Phys.* **A273**, 230 (1976).
- ⁷K. A. Erb, D. L. Hanson, R. J. Ascutto, G. B. Sherwood, J. S. Vaagen, D. A. Bromley, and J. J. Kolata, European Conference on Nuclear Physics with Heavy Ions, Caen, 1976 (unpublished), p. 34.
- ⁸G. Sherwood and R. J. Ascutto, *Bull. Am. Phys. Soc.* **22**, 40 (1977).
- ⁹D. Bachner, R. Santo, H. H. Duhm, R. Bock, and S. Hinds, *Nucl. Phys.* **A106**, 577 (1968).
- ¹⁰O. Häusser, D. Pelte, J. K. Alexander, and H. C. Evans, *Nucl. Phys.* **A150**, 417 (1970); P. M. S. Lesser, D. Cline, Ph. Goode, and R. N. Horoshko, *ibid.* **A190**, 597 (1972).
- ¹¹B. Haas, J. Chevallier, J. Britz, and J. Styczen, *Phys. Rev. C* **11**, 1179 (1975).
- ¹²S. L. Tabor and R. W. Zurmuhle, *Phys. Rev. C* **10**, 35 (1974).
- ¹³Z. P. Sawa, J. Blomqvist, and W. Gullhommer, *Nucl. Phys.* **A205**, 257 (1973).
- ¹⁴J. D. McCullen, B. F. Bayman, and L. Zamick, *Phys. Rev.* **134**, B515 (1964); J. N. Ginocchio and J. B. French, *Phys. Lett.* **7**, 137 (1963); J. N. Ginocchio, Ph.D. thesis, Univ. of Rochester, 1964 (unpublished); J. N. Ginocchio, *Nucl. Phys.* **63**, 449 (1965).
- ¹⁵F. B. Malik and W. Scholz, *Phys. Rev.* **150**, 919 (1966); W. Scholz and F. B. Malik, *ibid.* **153**, 1071 (1967).
- ¹⁶G. B. Sherwood, Ph.D. thesis, Yale Univ., 1978 (unpublished).
- ¹⁷J. V. Maher, D. A. Sink, T. J. Lewis, J. C. Peng, C. M. Cheng, and H. S. Song, in *Proceedings of the International Conference on Reactions between Complex Nuclei*, Nashville, Tennessee, 1974, edited by R. L. Robinson, R. K. McGowan, J. B. Ball, and J. H. Hamilton (North-Holland, Amsterdam, 1974), Vol. I, p. 56.
- ¹⁸A. J. Baltz, P. D. Bond, J. D. Garrett, and S. Kahana, *Phys. Rev. C* **12**, 136 (1975).
- ¹⁹J. L. Yntema and G. R. Satchler, *Phys. Rev.* **161**, 1137 (1967).
- ²⁰J. Styczen, J. Chevallier, B. Haas, N. Schulz, P. Taras, and M. Toulemonde, *Nucl. Phys.* **A262**, 317 (1976).
- ²¹R. A. Chatwin, J. S. Eck, D. Robson, and A. Richter, *Phys. Rev. C* **1**, 795 (1970).
- ²²A. Gobbi, R. Wieland, L. Chua, D. Shapira, and D. A. Bromley, *Phys. Rev. C* **7**, 30 (1973).
- ²³D. J. Pullen, B. Rosner, and O. Hansen, *Phys. Rev.* **166**, 1142 (1968).